The 6th International Conference on
Structural Health Monitoring of Intelligent Infrastructure
Hong Kong | 9-11 December 2013

WIRELESS SENSOR NETWORK POWERED BY DYE-SENSITIZED SOLAR CELLS

Roman Klis and Eleni Chatzi
Department of Civil, Environmental and Geomatic Engineering, ETH Zürich, Switzerland.
Email: klis@ibk.baug.ethz.ch

ABSTRACT

Wireless sensor networks technology (WSN) form a promising candidate for enabling the deployment of dense and relatively cheap sensor arrays. However, energy self-sustainability of wireless sensors remains a central issue withholding this technology from applicability into the industry and monitoring community. This problem is even more significant when the nodes of the network are used for acceleration sensing, in this case requiring both high sampling rates and excessive data transmission costs. The presented work investigates the usage of dye-sensitized solar cells combined with data compression techniques for obtaining self-sustainability of WSN nodes utilized for acquiring acceleration measurements. In the experimental setup the wireless nodes are coupled with the solar cells via a custom power conversion circuit. The circuit utilizes a large size super-capacitor used in place of a conventional battery solution. The designed power circuit supplies an Imote2 WSN node selected as a testing platform in this particular experiment. The software designed for the Imote2 node is able to perform measurement execution, data compression as well as communication tasks with other WSN nodes. The data transmission reduction scheme relies on incorporating the knowledge of structural behavior into the transmitted information. The efficacy and long-term applicability of such a solution for vibration-based monitoring of infrastructure is assessed via an experimental implementation on a simple cantilever model in the laboratory.

KEYWORDS

Wireless Sensor Networks (WSN), dye-sensitized solar cells, sensor sustainability, Imote2 system, measurement scheduling, “smart” data compression.

INTRODUCTION

Wireless Sensor Networks are currently becoming an industry ready solution for monitoring applications. The use of wireless rather than tethered sensing networks offers tremendous advantages for Structural Health Monitoring (SHM) purposes as they are easily deployable and low-cost thus enabling the use of much denser sensor arrays on large civil structures. As such networks are still in their early stages of development, they unavoidably come with a rather significant power consumption cost, low computational capabilities on the node level and limited acquisition bandwidths. Consequently, the so far implemented solutions lack the capacity of handling tasks requiring high sampling frequencies, including vibrational analysis which is the tool required for monitoring purposes. This has led to the development of data compression schemes for better exploitation of the acquired information (Zimmerman and Lynch 2009)

The Structural Health Monitoring research community intensively explores possibilities to use solar powered WSN nodes for improving the energy sustainability of such wireless nodes. A good example for this kind of system was presented by Miller (Miller *et al.* 2010). In this work a battery operated Imote2 platform was combined with a solar panel and the resulting performance was tested in a real life deployment scenario. A more generic implementation, i.e. not involving any particular WSN node, was demonstrated by Le Cam (Le Cam *et al.* 2012). The group developed a smart power management circuit designated to charge battery from solar panels for powering up any type of Wireless Sensor Network node. One of few attempts to use super-capacitors for powering up Wireless Sensor Network nodes has been performed by Xiaofan (Xiaofan *et al.* 2005). The developed node, named Prometheus, combines a battery solution with a super-capacitor acting as a charging buffer for the batteries. The node was designed to perform within the context of environmental monitoring.

The discussed solutions were mostly utilizing rechargeable batteries or rechargeable batteries combined with super capacitors. The work presented herein investigates a twofold approach for increasing node efficiency. On the hardware level, a super-capacitor only solution is implemented for powering up the wireless sensor.

Secondly on the software level, a data transmission reduction algorithm is investigated for optimizing the amount of transmitted information from individual nodes thus lowering the power consumption demand.

WIRELESS SENSOR NETWORK DISCRIPTION

Hardware

The Imote2 Platform, utilized in this implementation, was commercially introduced in year 2007 by Crossbow. The main CPU is Intel's XScala PXA27x processor capable of operating in a vast frequency range, from 13MHz up to 416 MHz. Additionally, a power management chip - Dialog DA9030 is present on the board. The board is also equipped with an embedded wireless radio chip - CC2420. With a proper antenna device this enables a wireless communication in a range of up to 100m within the line of sight. The Imote2 Platform is supplied with an additional measurement board ITS400. The sensor board is equipped with a 3D MEMS accelerometer LIS3LV02DQ provided by STMicroelectronics. The accelerometer provides 12bit resolution 2g signal in all 3 directions. The board communicates with the accelerometer via digital SPI connection.

As part of this work, which also pertains to the hardware level, the Imote2 platform was coupled with a prototype custom made power supply circuit. The circuit combines both a high efficiency maximal power point tracker device (Triune Systems TS52003) responsible for charging a super-capacitor, and a Microchip MCP1640 synchronous step-up converter utilized for powering up the Imote2. The selected boost converter offers above 80% efficiency for loads operating in range of 1.0 mA to 100 mA at 3.3 V (Microchip, 2011). The block diagram of the developed solution is presented in Figure 1. The solar panel is connected to the power circuit using a zener diod protection. The purpose of that is to assure that the TS52003 chip is not surged once a solar panel operates below the specified absolute maximum ratings for the chip.

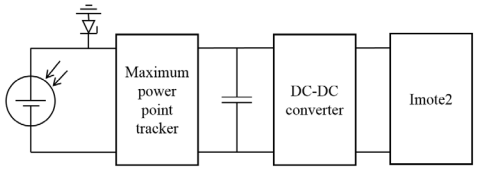

Figure 1. Block diagram of developed hardware solution

The selected solar panel is a novel Dye-Sensitized cell obtained from company G24i Power, ltd.

Software

The software which was implemented on the sensing nodes was written in TinyOS 2.0. It consists of a number of independent, event-driven tasks executed on the node level. The independence of the nodes is limited to securing an appropriate voltage level for the capacitor and requesting a wakeup time from the base station. The outline of the algorithm is described in the block diagram in the Figure 2. This software construction implies that the nodes of the network are fully dependent on the base-station master unit which is assumed to always be operational. The supervising software running on the base station has been implemented using a Python script installed on a Linux operating system.

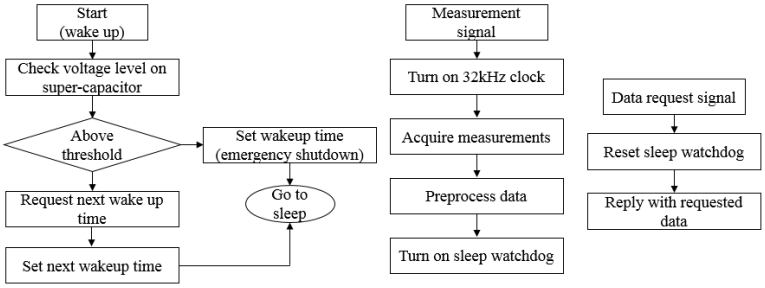

Figure 2. Flowchart of the software executed on the node level

DATA TRANSMISSION REDUCTION ALGORITHM (MR-UKF)

This is one of the key concepts introduced in this work toward sustainability of the sensing nodes. The idea behind the data transmission reduction algorithm relies on utilizing the knowledge of the underlying physical system for minimizing the necessary number of transmissions within the network and subsequently estimating the "missing data" by exploiting the underlying model. For this purpose the framework has been divided into two main modules/components. The first component is responsible for building the model from the obtained measurements by employing the System Identification (S-Id) tool described next. The second component utilizes the identified model in order to obtain estimates of system states and for predicting deviation from a previously, usually assumed "healthy", state of the structure.

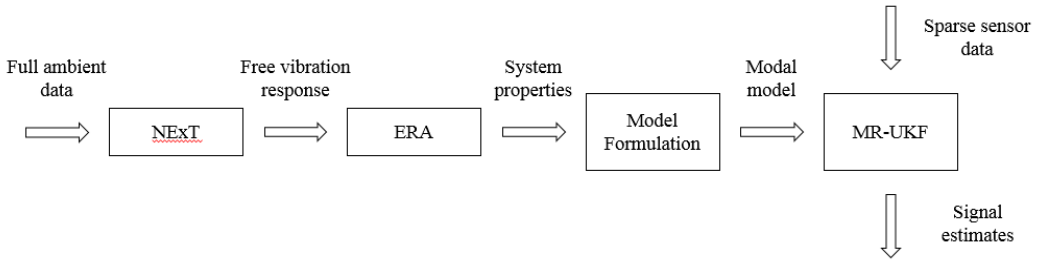

Figure 3. Data transmission reduction flowchart

The data transfer reduction algorithm is based on previous work conducted on the use of a UKF-ERA framework for SHM applications outlined in (Chatzi and Klis 2013). In that proposed framework the Eigensystem Realization Algorithm (ERA) is utilized in order to build a linear model of the system under the assumption that calibration measurements are performed using a dense sensor grid (initial phase). Next, this model is combined with the Unscented Kalman Filter (UKF) which acts as an estimator in presence of limited sensor readings. This is assumed to correspond to the operational phase of the monitoring system where fewer sensors are left in place.

In the work presented herein, that framework is extended for use with the wireless Imote2 nodes. The data flow within framework is illustrated in Figure 3. At an initial stage the Natural Excitation Technique (NExT) is employed in order to treat data that corresponds to ambient vibration and recover a free vibration response. The response signals are then processed using the ERA algorithm and the obtained system properties serve as a building block for the underlying system model formulation. The challenge arising herein is related to the sparse data obtained from the WN sensors at various, or rather non-constant sampling rates. This "data fusion" feature is handled here by using a Multi-Rate variant of the Unscented Kalman Filter (MR-UKF) fed with a state space modal model.

For a detailed description of the implemented methods, the interested reader is referred to existing literature on each methodology, namely for the UKF (Julier and Uhlmann 1997), the ERA (Juang and Pappa 1985), the NExT (Caicedo *et al.* 2004), and the MR-UKF (Armesto and Tornero 2004). The next section outlines the model formulation for use with the MR-UKF filter.

Model Formulation

The model assumes that the dynamics of the underlying system are governed by a set of N continuous-time forced equations of motion i.e. one per sensing unit:

$$[M]_{N\times N}[\ddot{z}(t)]_{N\times 1}+[C]_{N\times N}[\dot{z}(t)]_{N\times 1}+[K]_{N\times N}[z(t)]_{N\times 1}=[f(t)]_{N\times 1} \quad (1)$$

In the Eq. 1 M, C, K denote the mass, damping and stiffness matrix, $z(t)$ designates displacment and $f(t)$ is the external forcing. As outlined further in (Chatzi and Klis 2013), two methodologies can be employed in order to obtain a (reduced-order usually) model of the system.

Utilizing a modal model

This can be achieved by introducing the modal coordinate system $[u]_{K\times 1} = [\Phi]_{N\times K}[z]_{N\times 1}$ and multiplying Eq. 1 by $[\Phi]^{\Diamond}_{N\times K}$, where $[^{\Diamond}]$ indicates the pseudo-inverse operator:

$$\begin{aligned}&[\Phi]^{\Diamond}_{N\times K}[M]_{N\times N}[\Phi]_{N\times K}\ [\ddot{u}(t)]_{K\times 1} + \ldots\\ &[\Phi]^{\Diamond}_{N\times K}[C]_{N\times N}\ [\Phi]_{N\times K}\ [\dot{u}(t)]_{K\times 1} + \ldots\\ &[\Phi]^{\Diamond}_{N\times K}[K]_{N\times N}\ [\Phi]_{N\times K}\ [u(t)]_{K\times 1} = [\Phi]^{\Diamond}_{N\times K}[f(t)]_{N\times 1}\end{aligned} \tag{2}$$

In the Eq. 2 Φ is an $N\times K$ element eigenvector matrix formed from K, $N'th$ length modal vectors. This formulation demands that the Φ matrix is formed from modes that are mass-normalized. This is generally possible only in instances where some assumption on the mass may be formulated. In this work, this approach is utilized in the experimental setup examined in the applications section, where the mass distribution along the degrees of freedom of the structure is more or less known. A uniform mass distribution is chosen therein, corresponding to a diagonal mass matrix:

$$\mathrm{M} = \sum_{i=1}^{N} m_i\ ,\ m_i = \frac{\mathrm{M}}{N}\ ,\ [M]_{N\times N} = diag(m_1, m_2, ..., m_N) \tag{3}$$

Once this assumption is employed the eigenvectors can be then mass-normalized:

$$[\bar{v}_i] = \frac{[v_i]}{\sqrt{[v_i]^T[M][v_i]}}\quad i = 1\ldots N \tag{4}$$

Therefore the mass-normalized eigenvectors matrix is obtained $[\overline{\Phi}]_{N\times K}$ and used in Eq. 2. Due to the none-square eigenvector matrix, the mass-orthogonally property holds only approximately. Therefore Eq. 2 has to be reformulated as:

$$I_{K\times K}[\ddot{u}(t)]_{K\times 1} + [\Gamma]_{K\times K}[\dot{u}(t)]_{K\times 1} + [\Omega^2]_{K\times K}\ [u(t)]_{K\times 1} = [\overline{\Phi}]^{\Diamond}_{N\times K}[f(t)]_{N\times 1} + [e]_{K\times 1} \tag{5}$$

Where $I_{K\times K}$ is the identity matrix, Γ is the modal damping matrix, Ω^2 is the eigenvalues matrix and e is the error vector introduced by matrix pseudo-invers operation. At this stage the damping and eigenvalue matrix can be fitted with values obtained from identification part. By introducing state variables $x_1 = u, x_2 = \dot{u}$ and by forming a continues-time state-space modal model from Eq. 5 one obtains a following derivation:

$$\begin{bmatrix}\dot{x}_1\\ \dot{x}_2\end{bmatrix}_{2K\times 1} = \begin{bmatrix}\mathrm{O}_{K\times K} & I_{K\times K}\\ -\Omega^2_{K\times K} & -\Gamma_{K\times K}\end{bmatrix}\begin{bmatrix}x_1\\ x_2\end{bmatrix}_{2K\times 1} + \begin{bmatrix}\mathrm{O}_{N\times K}\\ \overline{\Phi}^{\Diamond}{}_{N\times K} + e_{K\times 1}\end{bmatrix}[f(t)]_{N\times 1} \tag{6}$$

By performing Euler integration on Eq. 6 one obtains a simple discrete time state-space equation of motion:

$$[x_{i+1}]_{2K\times 1} = [x_i]_{2K\times 1} + dt\left(\begin{bmatrix}\mathrm{O}_{K\times K} & I_{K\times K}\\ -\Omega^2_{K\times K} & -\Gamma_{K\times K}\end{bmatrix}[x_i]_{2K\times 1}\right) + dt\left(\begin{bmatrix}\mathrm{O}_{N\times K}\\ \overline{\Phi}^{\Diamond}{}_{N\times K} + e_{K\times 1}\end{bmatrix}[f_i]_{N\times 1}\right); x = \begin{bmatrix}x_1\\ x_2\end{bmatrix} \tag{7}$$

Eq. 7 is used in this framework for describing the dynamics of the discovered system as it is suitable for online implementation. One should observe that the force f_i component in the above equation is simulated as a zero mean white Gaussian noise distribution. This is accounted for in the UKF framework by assuming a process noise level of the order of the force contribution. This can easily be performed during the training period of the system. Since all the observations are performed on acceleration signals, the measurement equation can be obtained directly from the equation of motion:

$$[\ddot{z}]_{N\times 1} = [\overline{\Phi}]^{\Diamond}_{N\times K}\left[-[\Gamma]_{K\times K}[x_2]_{K\times 1} - [\Omega^2]_{K\times K}\ [x_1]_{K\times 1} + [\overline{\Phi}]^{\Diamond}_{N\times K}[f(t)]_{N\times 1} + [e]_{K\times 1}\right] \tag{8}$$

The complete model utilized by the MR-UKF filter is formulated in the following way:

$$x_{i+1} = [x_i]_{2K\times 1} + dt\left(\begin{bmatrix} \mathrm{O}_{K\times K} & I_{K\times K} \\ -\Omega^2_{K\times K} & -\Gamma_{K\times K} \end{bmatrix}[x_i]_{2K\times 1}\right) + w_k; x = \begin{bmatrix} x_1 \\ x_2 \end{bmatrix}$$
$$y_i = \left[\overline{\Phi}\right]^{\Diamond}_{N\times K}\left[-[\Gamma]_{K\times K}[x_2(i)]_{K\times 1} \; -\left[\Omega^2\right]_{K\times K} \; [x_1(i)]_{K\times 1}\right] + \eta_k \tag{9}$$

Utilizing ERA identified discrete model

Instead of using the modal information (natural frequencies and mode shapes) and damping ratios extracted from the ERA in order to build a modal model of the system, a more straightforward approach can be utilized. The discrete system matrices A_d, C_d which are readily obtained through the ERA method (Juang and Pappa 1985), can be utilized in order to obtain a model of the system. It needs to be noted that in this case as well, the state space system coordinates are no longer the physical system coordinates but instead some transformation (similar to vector u of the previous formulation):

$$\tilde{x}_{i+1} = A_d\left[\tilde{x}_i\right]_{2K\times 1} + \tilde{w}_k, \; \tilde{x}: \text{ERA coordinates (non-physical)}$$
$$y_i = C_d\left[\tilde{x}_i\right]_{2K\times 1} + \tilde{\eta}_k \tag{10}$$

This obviously constitutes a far more compact formulation and no assumption regarding the mass distribution or even the extracted damping needs to be made.

Multi-Rate Implementation

The innovation in the proposed scheme and one of the major components for regulating data transmission is the fact that data is not transmitted at a fixed sampling rata but rather in more sparse patterns, defined in what follows by means of a suitable *transmission matrix*. In this sense, the formulated state-space model is taken into account in order to recover "missing information" from the sensors as they transmit data in sparser regimes leading to a reduction in transmission costs. The amount of information transmitted from each sensor is quantified by using a suitable index, namely the *filling factor*, described in the numerical simulation section which is described next.

The Multi-Rate UKF algorithm employed herein (MR-UKF) is able to handle data transmitted at diverse sampling rates by simply performing the measurement update step of the Kalman Filter framework only for the amount of data available at a given point of the analysis. This process has successfully been demonstrated in (Smyth and Wu 2007) where a Multi-Rate linear KF was used for the fusion of acceleration and displacement data obtained at different sampling rates.

In order to validate the usability of the proposed scheme numerical simulations were firstly performed as described in the following section.

NUMERICAL SIMULATIONS

The synthetic model of an 18dof mass-spring-dashpot (discrete) system has been selected as the test-case for numerical simulations. A limited number of those DOFs, namely [1,3,5,7,9,12,15,17] where assumed as instrumented with the wireless accelerometer sensors. Next, the system was driven with a broadband white noise excitation applied to the fifth and twelfth node (or equivalent discrete DOF).

$$\begin{bmatrix} m_1 & 0 & \dots & 0 \\ 0 & m_2 & & 0 \\ \vdots & & \ddots & \\ 0 & 0 & & m_{18} \end{bmatrix}_{18\times18} \left[\ddot{z}(t)\right]_{18\times1} + \begin{bmatrix} c_1+c_2 & -c_2 & \dots & 0 \\ -c_2 & c_2+c_3 & & 0 \\ \vdots & & \ddots & -c_{18} \\ 0 & 0 & -c_{18} & c_{18} \end{bmatrix}_{18\times18} \left[\dot{z}(t)\right]_{18\times1} + \dots$$
$$\begin{bmatrix} k_1+k_2 & -k_2 & \dots & 0 \\ -k_2 & k_2+k_3 & & 0 \\ \vdots & & \ddots & -k_{18} \\ 0 & 0 & -k_{18} & k_{18} \end{bmatrix}_{18\times18} \left[z(t)\right]_{18\times1} = \left[f(t)\right]_{18\times1} \tag{11}$$

The synthetic model is governed by the Eq. 11. For the numerical simulation both the mass and stiffness per degree of freedom were selected as uniform ($m_i = 1e8, \mathrm{k_i} = 5e9$). The damping matrix was composed by assuming modal damping ratios in the range of .5-3%, which are linearly increasing for higher modes. The numerical simulations were performed with a frequency of $f_s = 100\ Hz$. The obtained response signals of the system were contaminated with a 10% RMS noise to signal ratio, in order to account for measurement noise, and were then fed in the ERA-NExT schema. The identification results are shown below in Figure 4. The plotted results indicate a quite satisfactory performance in capturing the natural frequency and associated modes.

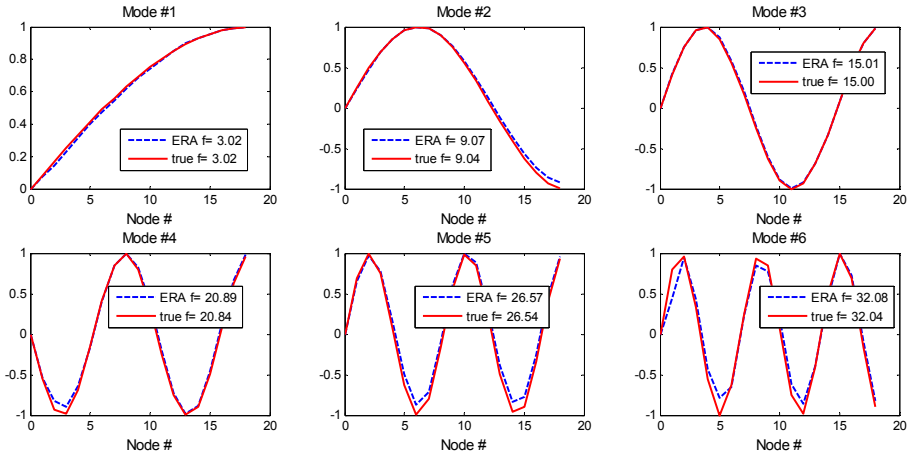

Figure 4. Modal shapes, reference and identified

The discrete matrices obtained from the ERA were utilized for setting up a reduced order model of the system, comprising 6dofs instead of 18, as shown in Eq. 9 of the previous section. The initial identification relies on a training period of fully transmitted information. Next, the capacity of MR-UKF for recovering the original signals from only partly transmitted data and limited observations is investigated. In order to gain some insight into which components of the full data are transmitted, a binary $M^t_{N\times L}$ *transmission matrix* is formulated. The matrix denotes the temporal and spatial (per-channel) localisation of the samples in the measured signal. Additionally a *filling factor* F_f is defined describing the volume of transmitted data i.e. a higher index corresponds to more transmitted samples. In order to assess the quality of reconstructions a simple Root Mean Square Error measure is employed between the estimates obtained from MR-UKF schema and the full signals.

$$F_f = \frac{\sum_{i=1}^{N}\sum_{j=1}^{L} M_{ij}^{\ s}}{N\times L};\ RMSE = \sqrt{\sum_{i=1}^{L}\left(\tilde{z}_i - z_i\right)^2} \tag{12}$$

In Eq. 12 $\tilde{z}_i$ indicates the estimate obtained from MR-UKF filter at a given time instance whereas L stands for the overall number of samples taken per channel during the measurement.

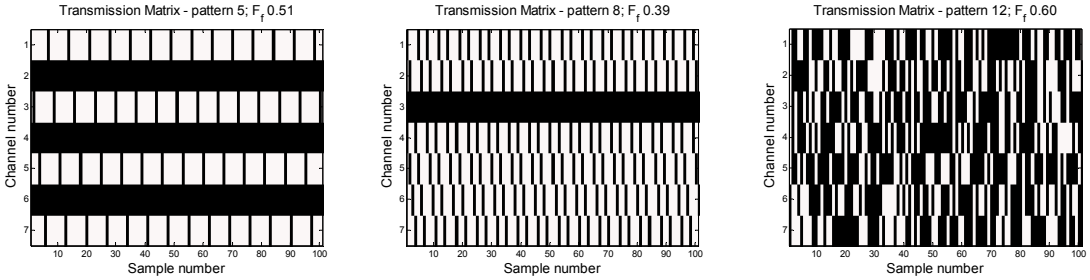

(a) (b) (c)

Figure 5. Exemplary transmission matrices

Figure 5 illustrates some of the transmission matrices generated for data recovery. The black colour indicates transmissions of the selected sample. Figures 5-a and 5-b show the example of empirically selected transmission matrices whereas Figure 5-c shows an example of a randomly generated pattern. It should be noted that the empirically selected transmission matrices assume that some of the channels perform full transmission. This was employed due to the fact that modal coordinates used in model formulation may only provide a spatial correlation i.e. they miss temporal dependencies. In order to account for this, it could prove beneficial for transmission matrices to include some selected complete temporal datasets.

Signal Recovery Results

Figure 6 presents extracts from recovered acceleration signals for different F_f values. Figure 7 summarizes the error estimation obtained by employing the RMS metric on each tested transmission matrix. Transmission patterns designated with the symbol *"R"* in Figure 7 were generated randomly.

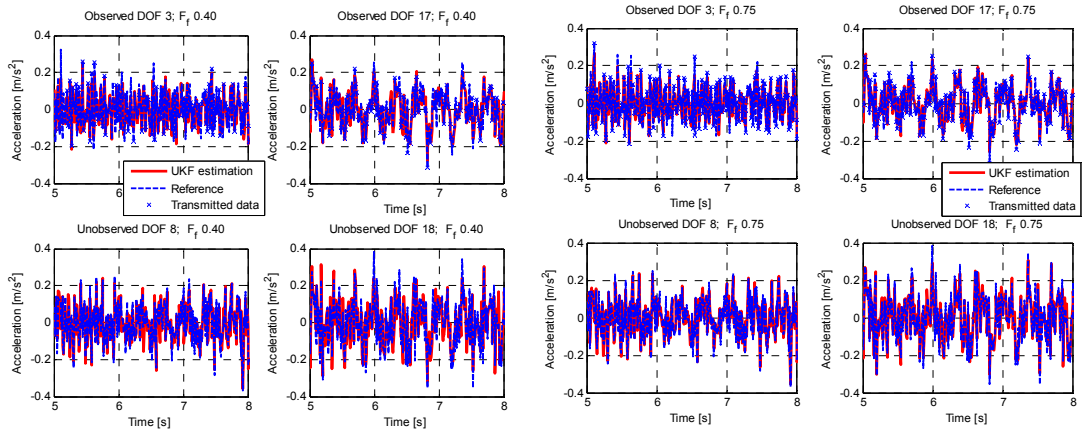

Figure 6. Reconstruction results for different *filling factor* values

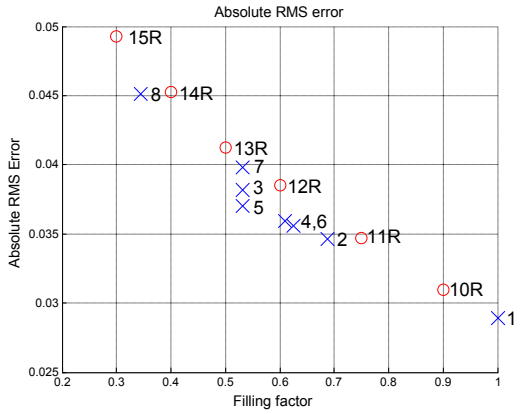

Figure 7. Summary of the RMS error analysis performed for different transmission matrices

Figure 7 depicts the RMS error of the MR-UKF signal estimation for both different filling factor values and different transmission matrix types. The RMS error values marked in the figure with a cross correspond to empirically selected transmission matrices whereas the values indicated with a circle correspond to RMS error values for randomly generated transmission matrices. It can be observed that the RMS error for random patterns is larger than the one of the empirical transmission matrices. This indicates the MR-UKF sensitivity to both the spatial and temporal distribution of transmitted samples in the signal. In the empirically selected patterns one to three "binding channels" are selected, i.e. sensors with continual data transmission. The reason for this selection is that the model used by the MR-UKF filter incorporates spatial correlations (through the eigenvectors) but misses the higher temporal dependencies. In other words, the model can only predict the next step response based on knowledge of the current time step. Once the filter is fed with few selected complete time histories, as in case of the empirically generated transmission matrices, performance is significantly enhanced.

EXPERIMENTAL SETUP

Figure 8 presents the experimental setup used in tests, simulating a simple setup of a continuous cantilever beam. The tests were conducted on a 2 meter long aluminium U shaped cantilever. The beam was instrumented with five wireless sensors and a co-located high accuracy wired sensing system.

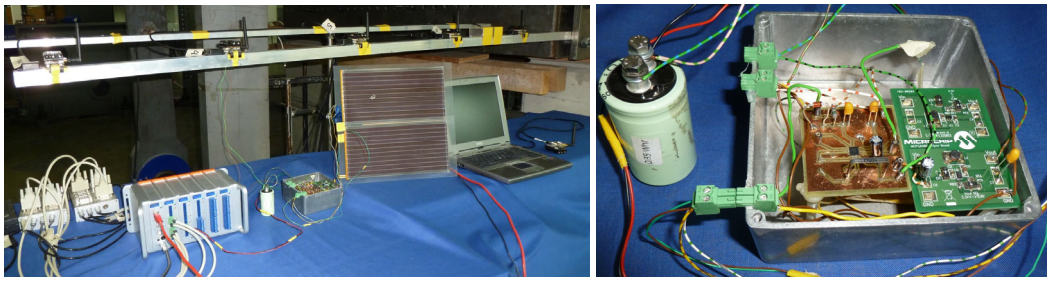

(a) Laboratory setup (b) Prototype circuit

Figure 8. Experimental setup and charging circuit connected to the solar cell

For data logging from the reference system a commercial Programmable Data Acquisition (PAQ) unit was used. Figure 8 shows the PAQ in the lower-left part of the figure. The recording was triggered by a signal obtained from a designated WSN node. The software was recording both acceleration and voltage drop down on the super-capacitor. For acquiring data from the WSN a laptop connected to a gateway node of the network was used. The designated node of the network was powered up from a custom-made charging circuit show in the Figure 8. The charging circuit was coupled with a dye-cell synthesised solar panel. In the experiments the structure was manually excited by tapping which was enough to simulate a broadband white-noise-like input force.

Table 1. Identified modal properties

Modal shape number	Reference system		Imote 2	
	f_n	ζ_n	f_n	ζ_n
1	5.50Hz	0.028	5.59 Hz	0.025
2	27.16 Hz	0.006	27.11 Hz	0.004
3	47.56 Hz	0.003	49.68 Hz	0.001
4	71.11 Hz	0.0059	71.30 Hz	0.036

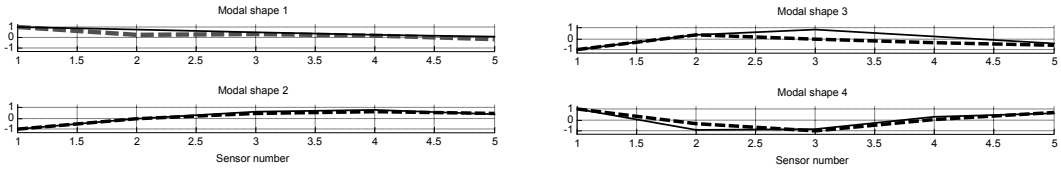

Figure 9. Identified modal shapes, reference (dashed) and Imote2 (black)

The identification was performed using the ERA-NExT technique. The results of the identification are presented in Figure 9 where the reference system is obtained by a parallel tethered network of higher accuracy MEMS

sensors. Based on the outcome, the modal model of the system was formulated as in Eq. 9. Next the MR-UKF schema was used for recovering the original signals from only partly transmitted data. For benchmark purposes the partial data transmission was simulated by extracting from the complete measurement time series only the samples indicated by the relevant *transmission matrix* pattern. Next the voltage drop down was recorded for both partially and fully transmitted signals.

RESULTS AND DISCUSSIONS

Figure 10 shows the resulting acceleration time series reconstructed from sparse data i.e. transmitted using a transmission matrix with a filling factor $F_f = 0.75$. A good correlation between estimated and reconstructed signals is observed.

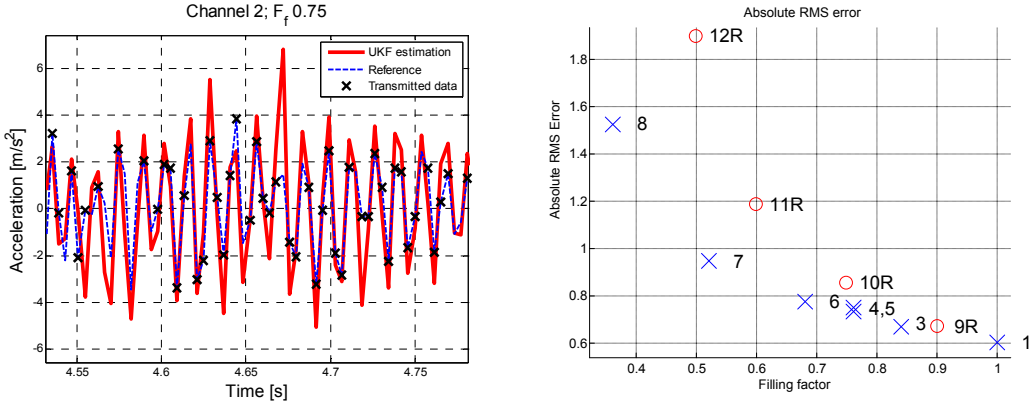

(a) Signal reconstruction (b) RMS error analysis

Figure 10. Acceleration signal reconstructions and RMS error analysis

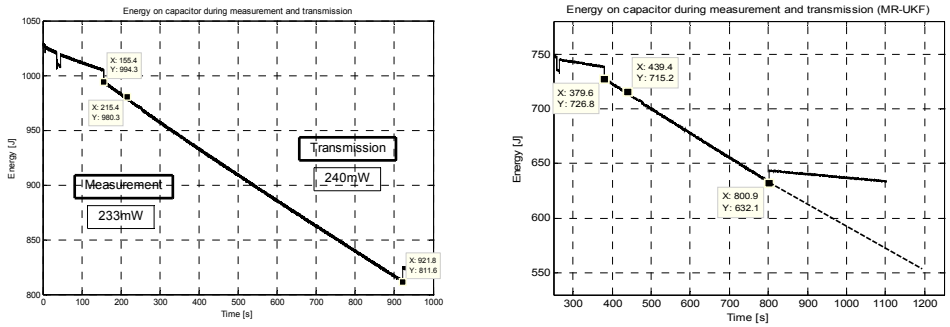

(a) Full transmission (b) Partial transmission

Figure 11. Discharge of the super-capacitor

Figure 11 compares the voltage discharge on the super-capacitor during measurement and data transmission state for complete and partial transmissions. One can notice that once the data transmission reduction framework is enforced the transmission time decreases. This results in shorter exposure to high power demand state.

CONCLUSIONS

The reduction of transmission overhead is critical for providing the self-sustainability of wireless sensors. The solution presented herein introduces an energy saving scheme for nodes operating via a highly constrained power source such as a super-capacitor.

The work demonstrates the possibility to operate an Imote2 node by merely using a super-capacitor based solution. Further works will focus on both the development of a generic power harvesting/external powering circuit platform for WSN nodes operating from super-capacitors and on the further enhancement of the Data Transmission Reduction Framework.

ACKNOWLEDGMENTS

This material is based upon work supported by the Swiss National Science Foundation under Research Grant "Implementation of Wireless Sensor Networks for Monitoring of Large Civil Structures", Swiss National Science Foundation (SNSF), project number 200021 143212.

REFERENCES

Armesto, L. and Tornero, J. (2004). "SLAM based on Kalman filter for multi-rate fusion of laser and encoder measurements", *Intelligent Robots and Systems 2004, Proceedings of 2004 IEEE/RSJ*, vol 2, 1860-1865, 28 Sept.-2 Oct.

Caicedo, J., Dyke, S. and Johnson, E. (2004). "Natural excitation technique and eigensystem realization algorithm for phase I of the iasc-asce benchmark problem: Simulated data", *Journal of Engineering Mechanics,* 130, 49–60.

Chatzi, E.N. and Klis, R. (2013). "Nonlinear System Identification using a UKF enhanced ERA framework", *11th International Conference on Structural Safety & Reliability*, June 16-20, Columbia University, New York, NY.

Chatzi, E.N. and Smyth, A.W. (2009). "The unscented kalman filter and particle filter methods for nonlinear structural system identification with non-collocated heterogeneous sensing", *Structural Control and Health Monitoring,* 16(1), 99–123.

Cui, D.Y., Xin, K.G., Spencer, B.F. and Liu, Y.F. (2012). "Decentralized NExT/ERA and RDT/ERA system identification in wireless smart sensor networks", *Applied Mechanics and Materials,* vol 204-208, 4946-4951.

Juang, J.-N. and Pappa, R.S. (1985). "An eigensystem realization algorithm for modal parameter identification and model reduction", *Journal of Guidance, Control, and Dynamics* 8(5), 620–627.

Julier, S.J. and Uhlmann, J.K. (1997). "A new extension of the kalman filter to nonlinear systems", *Proceedings of AeroSense: The 11th Int. Symposium on Aerospace/Defense Sensing, Simulation and Controls*, Orlando.

Le Cam, V., Le Maulf, R., Lemarchand, L., Martin, W. and Le Pen, M. (2012). "An optimized electronic device for solar power harvesting dedicated to wireless sensor networks", *6th European Workshop on Structural Health Monitoring* - Th.2.C.4.

Microchip (2011). *0.65V Start-up Synchronous Boost Regulator with True Output Disconnect or Input/Output Bypass Option*, 2011, Microchip, 23.01.2013, http://ww1.microchip.com/downloads/en/DeviceDoc/22234B.pdf

Miller, T.I., Spencer B.F., Li J. and Jo, H. (2010). *Solar Energy Harvesting and Software Enhancements for Autonomous Wireless Smart Sensor Networks*, NSEL Report Series

National Instruments (2011). *NI WSN Node Power and Performance Benchmarks*, 10.10.2011, National Instruments, 10.06.2013, http://www.ni.com/white-paper/9365/en

Smyth, A.W. and Wu, M., (2007). "Multi-rate Kalman filtering for the data fusion of displacement and acceleration response measurements in dynamic system monitoring", *Mechanical Systems and Signal Processing,* February 2007, 21(2), 706 – 72.

Triune Systems (2011). *High Efficiency SuperCap Charger for Photovoltaic Sources,* Triune Systems, 20.03.2013, http://www.mouser.com/ds/2/413/TS52003-2930.pdf

Xiaofan J., Polastre, J. and Culler, D. (2005). "Perpetual environmentally powered sensor networks", *Proceedings of the 4th International Symposium on Information Processing in Sensor Networks,* IPSN 2005, Article no. 65, 463-468, 15 April 2005.

Zimmerman, A. and Lynch, J.P. (2009). "A parallel simulated annealing architecture for model updating in wireless sensor networks", *IEEE Sensors Journal, IEEE*, 9(11), 1503-1510.